Activation of the small GTPases, rac and cdc42, after ligation of the platelet PAR-1 receptor

A. C. Azim, K. Barkalow, J. Chou, and J. H. Hartwig

Stimulation of platelet PAR-1 receptors results in the rapid (10 to 30 seconds) and extensive (30% to 40% of total) guanosine triphosphate (GTP) charging of endogenous platelet rac, previously identified as a possible key intermediate in the signal pathway between PAR-1 and actin filament barbed-end uncapping, leading to actin assembly. During PAR-1–mediated platelet activation, rac distributes from the cell interior to the cell periphery, and this reorganization is resistant to the inhibition of PI-3-kinase activity. Rac, in resting or activated platelets, is Triton X-100 soluble, suggesting that it does not form tight complexes with actin cytoskeletal proteins, though its retention in octylglucoside-treated platelets and ultrastructural observations of activated platelets implies that rac binds to plasma membranes, where it can interact with phosphoinositide kinases implicated in actin assembly reactions. PAR-1 stimulation also rapidly and extensively activates cdc42, though, in contrast to rac, some cdc42 associates with the actin cytoskeleton in resting platelets, and the bound fraction increases during stimulation. The differences in subcellular distribution and previous evidence showing quantitatively divergent effects of rac and cdc42 on actin nucleation in permeabilized platelets indicate different signaling roles for these GTPases. (Blood. 2000;95:959-964)

Introduction

The addition of thrombin to blood platelets causes them to spread lamellae. Massive actin polymerization is responsible for the mechanics of this change in shape. In working up the signaling pathways regulating this event from receptor activation to actin polymerization, we have obtained indirect evidence that the rho family GTPase rac, but not rhoA, becomes activated and channels information from the thrombin receptor, leading to actin assembly[1] (Tolias et al, unpublished data). Suitably permeabilized platelets maintain an intact signaling pathway between the thrombin receptor and an actin assembly-promoting reaction, the exposure of fast-growing (''barbed'') filament ends. Mutant N17rac1, which acts as a dominant negative inhibitory reagent for rac1, prevents thrombin from uncapping actin filament barbed ends in permeabilized platelets, whereas constitutively active V12rac1 promotes uncapping in the absence of thrombin-receptor stimulation. Inhibition of rhoA with C3 toxin does not reliably inhibit actin assembly in thrombin-reacted platelets,[2] and V12rhoA does not uncap actin filament barbed ends in permeabilized platelets.

The temporal relationship, however, between rac and cdc42 activation and platelet actin assembly reaction remains to be established. For rac and cdc42 to function in actin assembly as proposed, they must be activated before actin assembly and before the barbed-end nucleation reaction. Aggregated platelets have more detergent-insoluble cdc42 and rac than resting platelets,[3] suggesting that cell activation leads to a change in the function of cdc42 and rac that translocates them to the cytoskeleton. Rap1, a small GTPase, has also been shown to bind platelet cytoskeleton in aggregated platelets[4,5] and to be converted to its guanosine triphosphate (GTP) form.[6] The complexity of the aggregation reaction, which also involves secretion, shape change, and receptor modulation, makes the interpretation of the role of rac and cdc42 in actin assembly unclear.

In this article, we document directly and quantitatively the activation of platelet rac by thrombin receptor perturbation, as defined by its association with an effector polypeptide that only occurs when the GTPase has ligated GTP and by its spatial redistribution in the thrombin-treated platelet. We also show the activation of cdc42 by thrombin. Involvement of cdc42 in the thrombin-mediated actin assembly pathway appears to deviate from that of rac1, as evidenced by its movement into the Triton X-100-insoluble cytoskeleton.

Materials and methods

Materials

Human thrombin, wortmannin, bovine serum albumin, phallacidin, GTPγS, GTPβS, and other general chemicals were purchased from Sigma (St. Louis, MO). TRAP (SFLLRNPNQKYEPF) was purchased from BACHEM (King of Prussia, PA). Mouse anti-rac and rho monoclonal IgG antibodies were kindly provided by Dr Toshifumi Azuma (Brigham and Women's Hospital, Boston, MA). Mouse monoclonal cdc42 antibody was purchased from Transduction Laboratories (San Diego, CA). Horseradish peroxidase (HRP)–coupled antirabbit and antimouse antibodies were purchased from BIORAD (Hercules, CA). Secondary antibody for immunofluorescence was purchases from Jackson Immuno Research Laboratories (Bar Harbor, ME). All other antibodies were purchased from Sigma.

From the Division of Hematology, Brigham and Women's Hospital, Harvard Medical School, Boston, MA.

Submitted August 6, 1999; accepted September 30, 1999.

Supported by National Institutes of Health grants HL56252 and HL56949.

Reprints: J. H. Hartwig, Division of Hematology, Brigham and Women's Hospital, Harvard Medical School, Boston, MA 02115; e-mail: hartwig@calvin.bwh.harvard.edu.

The publication costs of this article were defrayed in part by page charge payment. Therefore, and solely to indicate this fact, this article is hereby marked "advertisement" in accordance with 18 U.S.C. section 1734.

Expression of GST-PAK1

The GTPase binding domain of PAK1 (amino acids 67-150) was inserted with the correct orientation into the pGEX-2T vector (Pharmacia, Piscataway, NJ). Dr G. Bokoch (Scripps Research Institute, La Jolla, CA) kindly provided the GST-PAK-1 cDNA. GST-PAK-1 was expressed in *Escherichia coli* and was affinity purified on a glutathione-Sepharose column. Cells were induced to express the fusion protein with 1 mmol/L isopropyl-thiogalactoside after 4 hours of growth in the log phase.

Preparation and treatment of platelets

Human blood from healthy donors was drawn into 1/10 volume of Aster-Jandel anticoagulant and centrifuged at 110*g* for 10 minutes. The platelet-rich plasma was removed and gel filtered at room temperature through a Sepharose 2B column, equilibrated, and eluted with a platelet buffer composed of 145 mmol/L NaCl, 10 mmol/L Hepes, 10 mmol/L glucose, 0.5 mmol/L Na_2HPO_4, 2 mmol/L KCl, 2 mmol/L $MgCl_2$, and 0.3% bovine serum albumin (BSA) (pH 7.4). Purified platelets were incubated for 30 minutes at 37°C to ensure a resting state. Platelet concentration was determined by a Coulter counter (Coulter, Miami, FL) and normally ranged from $2\text{-}3 \times 10^8$ cells per milliliter. Platelets were activated by the addition of 25 μmol/L TRAP or 1 U/mL thrombin. Wortmannin and LY294 002 treatments were performed at 37°C for 15 minutes at concentrations of 100 nmol/L and 25 μmol/L, respectively, before platelets were exposed to TRAP. Platelet activation was performed without stirring.

Immunofluorescent staining with anti-rac IgG

Platelets were activated by centrifugation onto glass coverslips at 250*g* for 5 minutes, as described previously,[7] and fixed with 2% formaldehyde in platelet buffer, pH 7.4, for 15 minutes at 37°C. Resting platelets were adhered to the coverslips by dilution into the 2% formaldehyde buffer; this was followed by centrifugation onto coverslips and fixation for 15 minutes. Fixed cells were permeabilized with 0.1% Triton X-100 containing 1 μmol/L fluorescein isothiocyanate (FITC)–phalloidin for 20 minutes, washed into PHEM buffer containing 0.3% BSA, and incubated with mouse anti-rac IgG for 1 hour at room temperature. Platelets were then washed, incubated with TRITC-rabbit antimouse IgG, washed again, incubated with 1 μmol/L FITC-phalloidin in the next-to-last wash step, and mounted for light microscopy. Stained cells were photographed on a confocal microscope.

Immunogold labeling of rac in platelet cytoskeletal preparations

Glass-adherent platelets were permeabilized with 0.75% Triton in PHEM buffer containing 0.1% glutaraldehyde or were mechanically disrupted by attaching a poly-lysine–coated coverslip to adherent cells and removing the coverslip (unroofed) in PHEM buffer.[8] Unroofed and permeabilized cells were fixed with 1% glutaraldehyde for 10 minutes at 37°C. The fixative was blocked with 0.1% sodium borohydride in PHEM buffer, 60 mmol/L PIPES, 25 mmol/L Hepes,10 mmol/L EGTA, 0.75% Triton X-100, pH 7.8. Coverslips containing cytoskeletons were washed twice with PHEM buffer, pH 7.8, and twice in the PHEM buffer containing 0.5% BSA. Coverslips were covered with a 10-μg/mL solution of mouse anti-rac IgG at room temperature for 1 hour and subsequently washed 3 times with PHEM/BSA. Coverslips were then treated for 1 hour with a 1:20 dilution of 8-nm gold particles coated with goat antimouse-IgG, washed 3 times in PHEM/BSA and 3 times in PHEM, and fixed with 1% glutaraldehyde in PHEM buffer. Samples were washed in distilled water, rapidly frozen, freeze dried, and coated with 1.4 nm tungsten-tantalum with rotation and 2.5 nm carbon without rotation. Replicas were recovered, picked up on carbon-formvar-coated copper grids, viewed, and photographed in a JEOL EX-1200 electron microscope at an accelerating voltage of 100 kV.

GTP-rac and GTP-cdc42 trapping assay

We based this method on principles established by Benard et al,[9] who measured GTPase activation in neutrophils. This assay uses the PAK-1 CRIB domain (amino acids 67-150) to trap GTP-bound rac and cdc42. Resting or activated platelets were lysed by the addition of 1/10 volume of a solution containing 10% Triton X-100, 500 mmol/L Tris-HCl, 50 mmol/L EGTA, 50 mmol/L EDTA, 52 nmol/L leupeptin, 10 nmol/L benzamidine, 123 nm aprotinin, and 10 μmol/L phallacidin or in a PHEM buffer used to analyze cytoskeletal structure.[10] Cytoskeletal and soluble-fluid fractions were separated by centrifugation of the lysate at 100,000*g* for 20 minutes. This soluble detergent fraction that followed ultracentrifugation will be referred to as high-speed supernatant. This high-speed supernatant was carefully removed and mixed with the Sepharose 4B-glutathione-GST-PAK1 bead conjugates for 4 to 8 hours at 4°C. Beads containing 10 to 20 μg recombinant GST-PAK1 were used for each assay. Precaution was taken to use fresh GST-fusion protein of PAK1. After the incubation period, the beads were collected by centrifugation at 10,000*g* for 5 minutes and washed with chilled TBS-Tween (0.1% Tween 20, 150 mmol/L NaCl, 20 mmol/L Tris-HCl, pH 7.5). SDS-PAGE sample buffer $5\times$ or $1\times$ was added to the supernatant fluid or the Sepharose bead pellet, respectively, to make the final volumes equal. The high-speed pellet was used to quantitate rac and cdc42 binding to the actin cytoskeleton. Bound rac and cdc42 were quantitated from the bead pellet by immunoblotting using anti-rac and anti-cdc42 antibodies. Rac and cdc42 were separated on 12% SDS-PAGE gels and subsequently transferred to polyvinylidene difluoride (PVDF) membranes for immunoblotting.

Polyacrylamide gel electrophoresis and immunoblot analysis

Proteins were electrophoresed as described by Laemmli[11] with some modifications. Samples were separated on 12% polyacrylamide gels and stained with 0.2% Coomassie brilliant blue. Immunoblotting was performed by electrophoretically transferring the proteins on PVDF Immobilon P membranes (0.45 μm; Millipore, Bedford, MA) in transfer buffer containing 20% methanol, 25 mmol/L Tris, and 195 mmol/L glycine. Membranes were blocked with 5% Carnation (Glendale, CA) nonfat dry milk in TBS-Tween 20 (20 mmol/L Tris, 150 mmol/L NaCl, 0.05% Tween 20). The blocked membrane was incubated with 1:1000 dilution of mouse rac and cdc42 monoclonal antibodies in TBS-Tween 20 buffer (containing Carnation 5% nonfat dry milk) overnight. Secondary mouse and rabbit HRP-coupled antibodies were used at a 1:3000 dilution in TBS-Tween buffer supplemented with 5% nonfat dry milk. Chemiluminescence detection was done using the Pierce system.

Results

Validation of rac and cdc42 trapping assay in platelets

Figure 1 shows the validity of this assay in platelets. After incubation with GTP or GTPγS, all the rac and cdc42 protein from

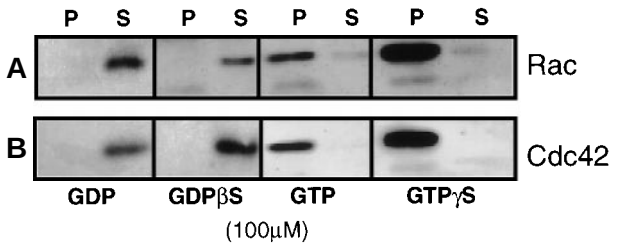

Figure 1. Demonstration of the specificity of the GST-PAK1-glutathione-Sepharose 4B-beads for the GTP forms of rac and cdc42. (A) Anti-rac immunoblot showing the effect of 100 μmol/L GDP, GTP, GDPβS, or GTPγS on the amount of rac collected from a 100 000*g* supernatant (high-speed supernatant) of detergent-lysed human platelets. (B) Anti-cdc42 immunoblot showing the amount of cdc42 trapped after loading high-speed supernatant with 100 μmol/L GDP, GTP, GDPβS, or GTPγS. Rac or cdc42 remaining in the supernatant (S) was separated from that which bound to beads by centrifugation at 10 000*g* for 2 minutes. The bead pellets (P) were washed with excess volume of TBS-Tween 20 buffer (pH 7.4) and denatured with SDS-sample buffer, bound protein displayed by 12% PAGE, and then were transferred to PVDF membrane for immunoblotting.

the high-speed supernatant bound to PAK1-coated beads, and no rac or cdc42 bound after loading with guanosine diphosphate (GDP) or GDPβS. This demonstrated that the binding of rac and cdc42 to the GBD domain of PAK1 required bound GTP to the GTPase.

TRAP stimulation causes translocation of cdc42 but not rac to the platelet cytoskeleton

We first had to determine the distribution of rac and cdc42 between the soluble-protein phase and the actin-based cytoskeletal fraction of resting and activated platelets. Platelets contained 1.9 to 3.1 and 0.21 μmol/L rac and cdc42, respectively. Insolubility of cdc42 and of rac has been reported after platelet aggregation.[3] In Triton X-100 high-speed supernatant prepared from resting platelets, the bulk of rac and cdc42 were soluble (90% to 100% of the total); no rac and only a small amount of the total cdc42 pellet were soluble with actin filaments at 100 000*g* from resting platelets (Figure 2). When platelets were activated with 25 μmol/L TRAP in the absence of aggregation, all the rac protein remained in the Triton X-100 supernatant (Figure 2A) and rac did not associate with F-actin in lysates from resting platelets after loading with GDP, GDPβS, GTP, or GTPγS (data not shown). This result demonstrated that the GTP charging of rac had only to be assayed in the Triton X-100 soluble high-speed supernatant. Although solutions containing Triton X-100 completely released rac from platelets, the platelet permeabilization scheme involving n-octyl β-D-glucopyranoside (OG) liberated only a small amount of rac, leaving most of the protein in the permeabilized platelet (Figure 2B). This finding was consistent with the retention of a signaling pathway involving rac in these platelet preparations. Approximately 30% of the total cdc42 co-sedimented with the Triton X-100-insoluble actin cytoskeleton after ligation of the PAR-1 receptor (Figure 2A). We determined whether the association of cdc42 with the cytoskeleton was affected by the bound guanine nucleotide. The incubation of platelet lysates with GTP and GTPγS significantly increased the sedimentation of cdc42, showing that the incorporation of cdc42 into the platelet cytoskeleton was facilitated by GTP (Figure 2C). Like rac, most of the cdc42 was not eluted when OG was used to permeabilize platelets (Figure 2B).

Thrombin and TRAP induce rapid activation of rac and cdc42 in platelets

When resting human platelets were activated with TRAP and then lysed in a Triton X-100 solution lacking magnesium to slow intrinsic GTPase activity and nucleotide exchange. GTP-bound rac was collected with GST-PAK1–Sepharose bead complexes. Rac bound to the PAK1-beads was visualized in immunoblots with an anti-rac monoclonal IgG (Figure 3A). As described above, little or no rac was collected in the GTP-bound state from resting platelets. However, after ligation of the PAR-1 receptor with 25 μmol/L TRAP, GTP-rac increased 6-fold in platelet high-speed supernatant (Figure 3A). The increase in GTP-rac content was rapid and peaked 30 to 60 seconds after the addition of TRAP to platelets. Although the extent of rac activation varied among platelet preparations, the kinetics of GTP-loading was similar in all experiments. In the best experiments, GTP-rac increased to 40% of the total rac contained in the high-speed supernatant. F-actin content increased with a similar time course after PAR-1 receptor ligation (data not shown). The loading of rac with GTP also was found in platelets activated with 1 U/ml of thrombin (Figure 3B).

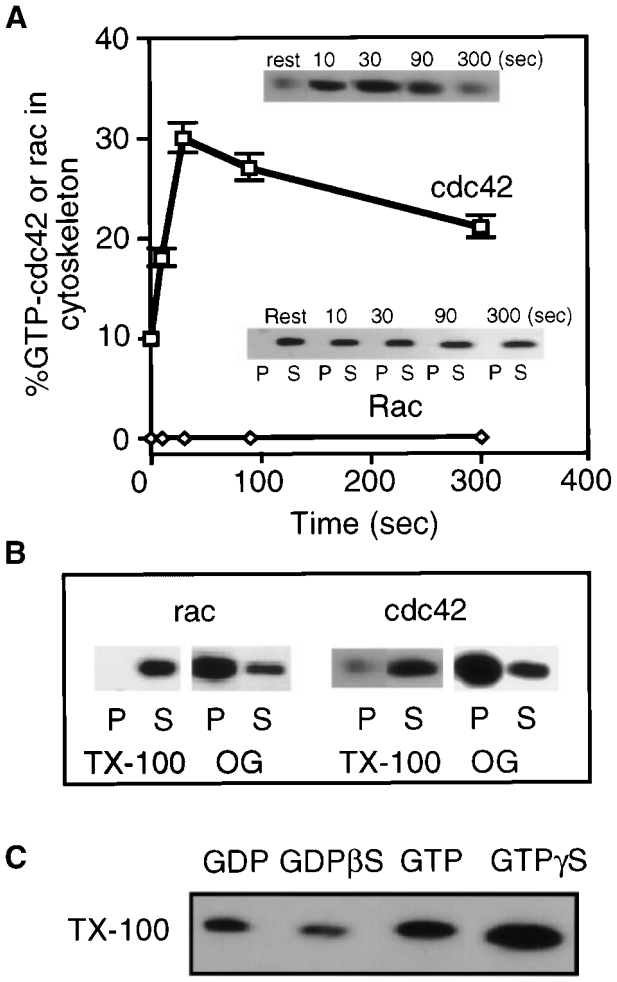

Figure 2. Distribution of rac and cdc42 in platelets after activation with 25 μm TRAP. Distribution of rac and cdc42 in platelets at rest and after activation with 25 μmol/L TRAP. Platelets were permeabilized with buffer containing Triton X-100. (A) Quantitation of the amount of rac or cdc42 that co-sediments with the actin-based cytoskeleton relative to the total. (top inset) Representative immunoblot showing the incorporation of cdc42 into the detergent insoluble cytoskeleton (100 000*g* pellet). (bottom inset) Immunoblot for rac in the high-speed supernatant (S) or pellet (P) from detergent lysates. (B) Distribution of rac and cdc42 in cytoskeletal pellet (P) or supernatant (S) from platelets permeabilized with buffers containing 0.1% Triton X-100 (TX-100) or 0.5% octyl-glucoside (OG). The bulk of rac and cdc42 are associated with the OG-insoluble material. (C) Effect of 100 μmol/L GDP, GTP, GDPβS, or GTPγS on the movement of cdc42 into actin cytoskeleton of platelets permeabilized with 0.1% TX-100.

As shown in Figure 4, TRAP activation of platelets led not only to increased cytoskeletal association but to a rapid increase in the amount of GTP-cdc42 measured in the 100 000*g* supernatant. Like rac, the increase in GTP-cdc42 was rapid and reached a maximal extent of approximately 6-fold at 30 seconds before it decreased. This increase was measurable within 10 seconds of TRAP or thrombin addition. The decrease in the amount of GTP-cdc42 recovered from supernatant corresponded in part to the incorporation of cdc42 into the platelet actin skeleton (Figure 2A). The kinetics of cdc42 charging (Figure 4) and movement into the cytoskeleton (Figure 2) are superimposable. The GTP-cdc42 content also increased 4- to 7-fold in the high-speed supernatant from platelets activated with thrombin (Figure 4B). Because GST-PAK1 bound to GTP-cdc42 and had no detectable binding to GDP-cdc42, we concluded that PAR-1 ligation increased cdc42 charging with GTP.

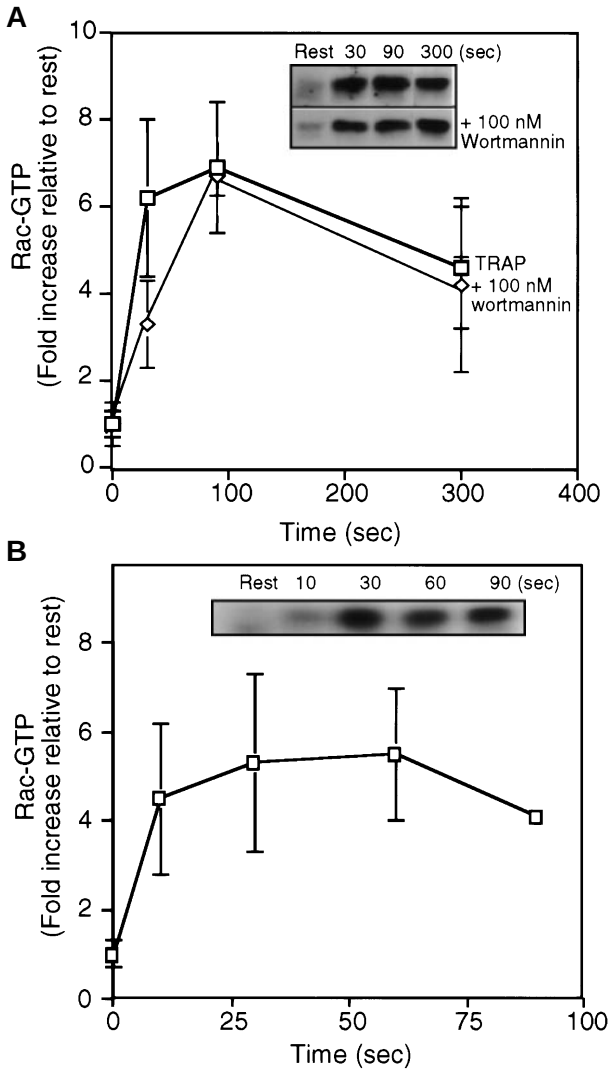

Figure 3. Quantitation of GTP-rac from high-speed supernatant prepared from resting platelets or platelets stimulated with 25 μmol/L TRAP in the presence or absence of PI-3-kinase inhibitor wortmannin or 1 U/mL thrombin. (A) Graph quantifying the increase in GTP-rac contained in the soluble fraction of lysates prepared from resting (rest) or TRAP-activated cells. The graph is an average of a minimum of 4 experiments (mean ± SD). Resting cells contained from 2% to 10% of the total rac. Activation increases the amount of GTP-rac by 6-fold to 30% to 40% of the total rac protein in the high-speed supernatant. GTP-rac formation after PAR-1 ligation is not affected by wortmannin. (inset) Representative anti-rac immunoblots of rac collected from high-speed supernatant of resting or TRAP activated platelets. GTP-bound rac was collected with the GBD-binding domain of PAK1 bound to Sepharose beads and is visualized in immunoblots (top) with an anti-rac mouse monoclonal antibody and a HRP-goat antimouse antibody. Platelets were incubated with 100 nmol/L wortmannin for 15 minutes before stimulation with TRAP (bottom). The amount GTP-rac collected and the kinetics of GTP-charging in the presence of 100 nmol/L wortmannin are similar to that in high-speed supernatant from cells activated without inhibitors. (B) Quantitation of the content of GTP-rac in high-speed supernatant from resting platelets and platelets activated using 1U/mL thrombin. (inset) In a representative experiment, the relative amount of GTP-rac collected using the PAK1-bead complexes.

Inhibition of PI-3-kinase does not affect rac charging with GTP in activated platelets

Actin assembly in lamellae induced by PAR-1 ligation in platelets is insensitive to the PI-3-kinase inhibitors, wortmannin, and LY294002.[12] However, wortmannin inhibits lamellipodia formation and ruffling in fibroblasts.[13] These results place PI-3-kinase upstream of rac in fibroblasts, a finding supported by GTP/GDP exchange measurements in PDGF-activated fibroblasts.[14] Hence, the effect of PI-3-kinase inhibition by wortmannin on the GTP charging of rac and cdc42 in platelets was determined. As shown in Figure 3A, treatment of platelets with wortmannin did not significantly change the kinetics or the extent of GTP-rac recovered with the PAK1-beads. The GTP charging of rac also was not affected in platelets treated with 50 μmol/L LY294002 (data not shown).

Rac moves into the membrane–cytoskeleton interface after platelet activation in a wortmannin-insensitive fashion

Figure 5 shows the distribution of rac in fixed and permeabilized platelets. In resting platelets, rac appeared uniformly distributed throughout the cell (Figure 5D). However, after activation, a

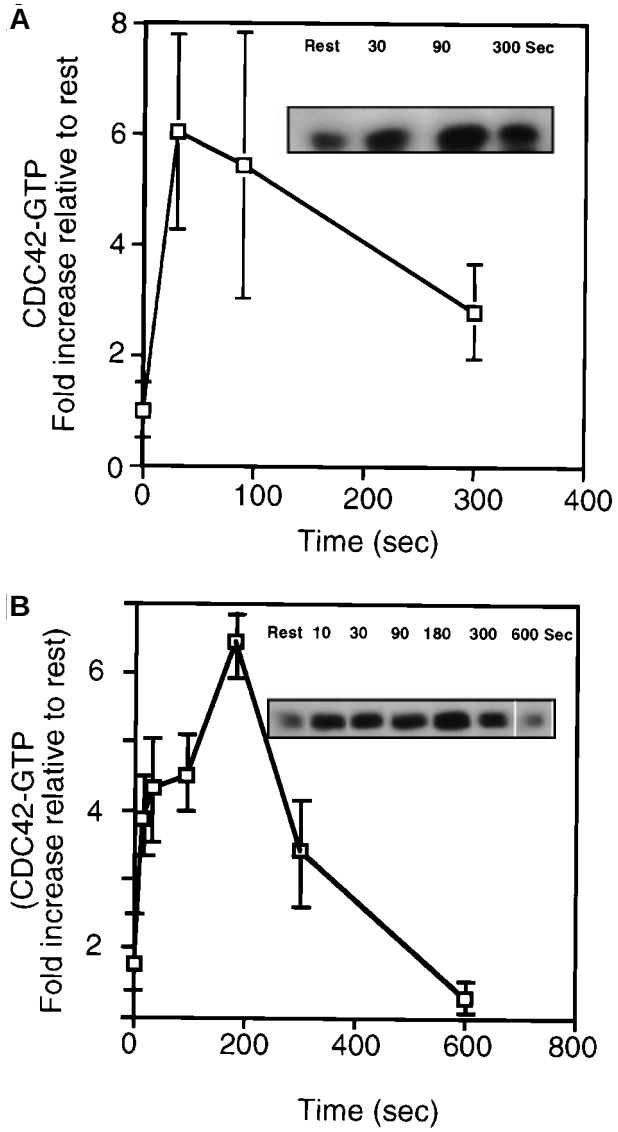

Figure 4. Quantitation of GTP-cdc42 from high-speed supernatant prepared from resting platelets or platelets stimulated with 25 μmol/L TRAP or 1 U/mL thrombin. (A) Measurement of GTP-cdc42 in high-speed platelet supernatant. The plot is an average of 4 experiments (mean ± SD). (inset) Representative anti-cdc42 immunoblot from resting or TRAP-activated cells (30 to 300 seconds). The graph shows that there is a 6-fold increase in the relative amount of GTP-cdc42 collected 30 seconds after TRAP activation. (inset) Representative immunoblot of cdc42 collected with the bead complexes. (B) Graph showing GTP-cdc42 after thrombin (1 U/mL) stimulation of platelets (n = 3, mean ± SD). (inset) Representative experiment of cdc42 bound to the beads in high-speed supernatant from resting or thrombin/TRAP activated cells.

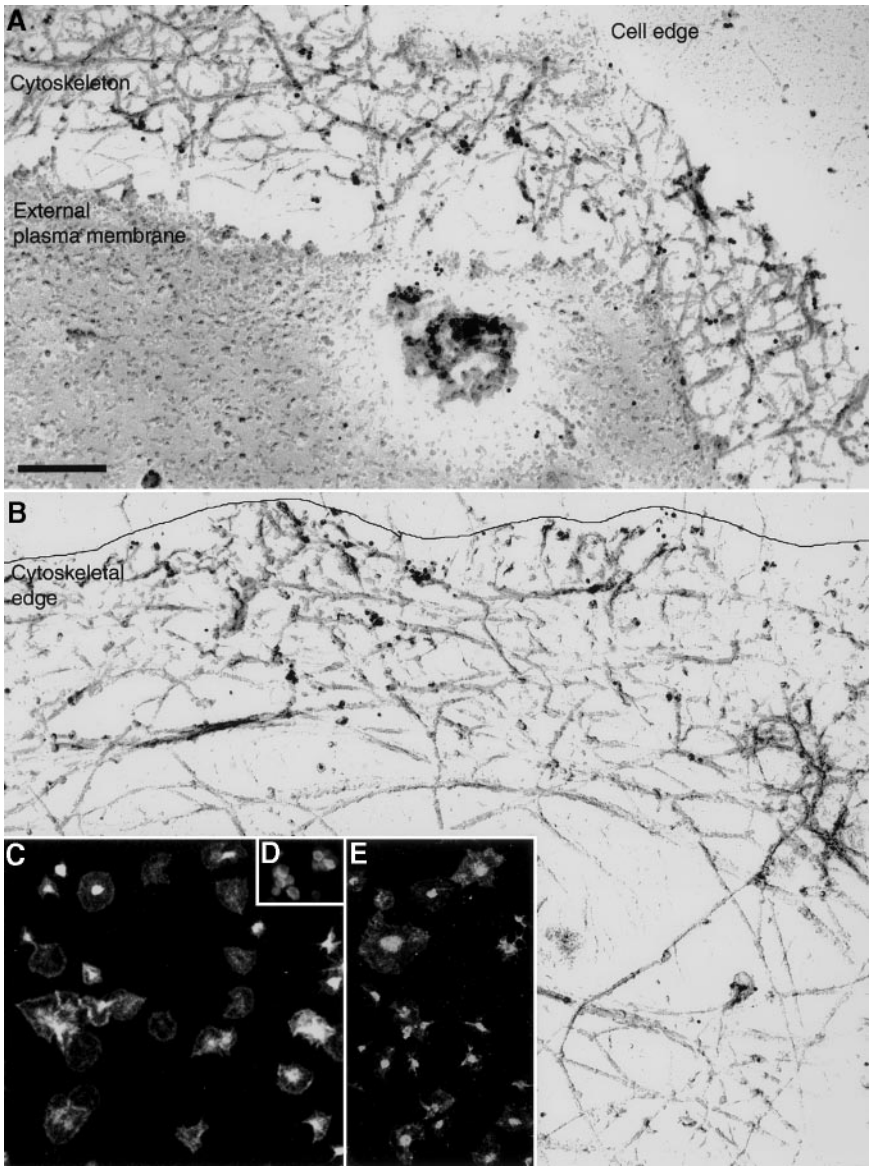

Figure 5. Localization of rac in resting and activated platelets. Immunogold localization of rac at the edge of cytoskeletal preparations from activated platelets. Rac was localized using a combination of mouse anti-rac IgG and 8 nm gold particles coated with goat antimouse IgG. Bar, 100 nm. (A) Representative cortical region from a mechanically unroofed platelet showing anti-rac gold, which locates near the margin of the cell in small clusters. Gold clusters are also found near the ends of actin filaments, where they appear to intersect residual plasma membrane. The apical plasma membrane is labeled. The line delineates the edge of the cytoskeleton. (B) Representative Triton X-100 detergent cytoskeleton showing the localization of rac. Anti-rac gold is localized along the edge of the actin cytoskeleton. (C) Distribution of rac in resting (D) and activated platelets (C,E) determined by immunofluorescence microscopy. Rac is visualized with mouse anti-rac IgG and TRITC-labeled donkey anti-mouse IgG. In resting platelets, rac is uniformly distributed. After activation, rac concentrates near the cell margins and in densities near the cell center. The movement of rac to the cell cortex is not affected by treatment of the platelets with wortmannin (E).

portion of the rac moved to the cell periphery and concentrated with actin filaments in lamellae and in extended processes such as filopodia. Rac also concentrated in the center of the platelet, which was enriched in platelet granules and membrane. Figure 5E shows that wortmannin treatment did not alter this redistribution of rac and that platelets spread in the presence of these inhibitors. To gain more information about rac contained within the platelet cortex, we localized rac in disrupted platelet preparations in the electron microscope. Because Triton X-100 eluted rac from unfixed platelets, we used 2 approaches to maintain rac in the platelet. First, platelets were mechanically unroofed in the absence of detergent (Figure 5A). This procedure revealed portions of cytoskeleton underlying removed membrane and protein-membrane interactions disrupted by detergents were maintained, allowing actin-membrane contacts to be visualized.[8] In unroofed platelets, 8 nm anti-rac gold particles bound along the edge of the cytoskeleton and along the residual plasma membrane. In the second procedure, we extracted cells with the detergent Triton X-100 in buffers containing 0.1% glutaraldehyde. Figure 5B shows that in a representative cytoskeleton, gold particles were predominately at the cytoskeletal edge.

Discussion

The reproducible and extensive temporal sequence of actin remodeling in platelets makes these cells useful for defining the steps linking rho family GTPases to particular morphologic responses involving actin rearrangements. This article adds direct measurements of rac activation to the previous indirect evidence implicating this GTPase in the pathway from thrombin receptor perturbation to actin assembly. Rac activation is rapid, peaks within 10 to 30 seconds of PAR-1 receptor ligation, and involves 30% to 40% of the total platelet rac protein. In permeabilized platelets, 5 to 10 nmol/L rac maximally activates actin filament barbed-end uncapping.[1] Because we found that platelets contain 2 to 3 μmol/L rac, the fraction of rac activated by thrombin was sufficient to produce the effects observed with exogenous active rac.

Inhibition of PI-3-kinase activity blocks some but not all actin assembly reactions. One of the exceptions is thrombin-mediated platelet actin polymerization.[12] The observation reported here that PI-3-kinase inhibitors had no effect on rac activation or subcellular

redistribution to the cell periphery is consistent with rac operating in platelets independently of D3 phosphoinositides. One clue to the differential sensitivity of actin-signaling reactions to D3 phosphoinositides may reside in whether signaling traffics to rac through D3 phosphoinositide-dependent or -independent upstream controls. Among these regulators is the protooncogene VAV, a GEF (GTPase exchange factor) for rac, which exists in D3 phosphoinositide-dependent (VAV1) or -independent (VAV2) isoforms.[15] We predict, therefore, that VAV2 is the conduit to signaling from PAR-1 to rac in platelets.

We also showed that PAR-1 ligation leads to cdc42 activation with a timing and magnitude approximating the GTP charging of rac. We have less information about the role of cdc42 than about rac in platelet actin assembly reaction. The evidence in this article suggests that cdc42 functions in different ways from rac, a conclusion consonant with the original discovery that rac and cdc42 induce different morphologies in Swiss 3T3 cells.[16-18]

Platelet rac is detergent soluble in resting and activated platelets, suggesting that it does not bind tightly to the actin cytoskeleton of nonaggregated cells. Rather, we think that activation targets it to membrane-bound lipid kinases that synthesize D4 phosphoinositides, which mediate actin filament barbed-end uncapping. The retention of rac in OG-treated platelets suggests a weak association of rac with membranes in resting and activated platelets. The localization of rac to membranes adjacent to actin filaments that elongate in thrombin receptor-activated platelets[19] is also consistent with the idea that rac interacts with membrane lipids to induce actin filament assembly. In contrast, cdc42 appears to bind to the actin cytoskeleton in resting platelets and, more so, in a GTP-dependent fashion, in activated platelets. This finding complements much evidence implicating cdc42 as facilitating the construction of multiprotein assemblies, including members of the WASp family, WASp-interacting proteins, and the ARP2/3 complex to initiate de novo nucleation and elongation of monomeric actin.[20-28] Further evidence that rac and cdc42 have different roles in platelets is that rac is much more potent than cdc42 in promoting actin filament nucleation activity in permeabilized platelets (Hartwig JH, unpublished data).

In conclusion, we have quantified GTP-rac and GTP-cdc42 in resting and thrombin-activated human platelets. The ligation of PAR-1 causes the charging of rac and cdc42 and temporally links GTPase activation to platelet responses. These experiments add to the wealth of information implicating rac and cdc42 as central proteins in the control of cell motility.

Acknowledgments

We thank Dr Gary Bokoch for the PAK1 cDNA and Dr Thomas P. Stossel for insightful criticism. We also thank Dr Joseph Italiano for his continued moral support.

References

1. Hartwig J, Bokoch G, Carpenter C, et al. Thrombin receptor ligation and activated Rac uncap actin filament barbed ends through phosphoinositide synthesis in permeabilized human platelets. Cell 1995;82:643-653.
2. Leng L, Kashiwagi H, Ren X-D, Shattil S. RhoA and the function of platelet integrin αIIbβ3. Blood. 1998;91:4206-4215.
3. Dash D, Aepfelbacher M, Siess W. Integrin aIIbβ3-mediated translocation of CDC42Hs to the cytoskeleton in stimulated human platelets. J Biol Chem. 1995;270:17,321-17,326.
4. Fischer TH, Gatling M, Duffy CM, White GC. Incorporation of Rap 1b into the platelet cytoskeleton is dependent on thrombin activation and extracellular calcium. J Biol Chem. 1994;269: 17,257-17,261.
5. Fischer T, Gatling M, Laca J-C, White G. Rap1B, a cAMP-dependent protein kinase substrate, associates with the platelet cytoskeleton. J Biol Chem. 1990;265:19,405-19,408.
6. Franke B, Akkerman J-W, Bos J. Rapid Ca^{2+}-mediated activation of Rap1 in human platelets. EMBO J. 1997;16:252-259.
7. Hartwig J. Mechanism of actin rearrangements mediating platelet activation. J Cell Biol. 1992; 118:1421-1442.
8. Hartwig J, Chambers K, Stossel T. Association of gelsolin with actin filaments and cell membranes of macrophages and platelets. J Cell Biol. 1989; 108:467-479.
9. Benard V, Bohl B, Bokoch G. Characterization of rac and cdc42 activation in chemoattractant-stimulated human neutrophils using a novel assay for active GTPases. J Biol Chem. 1999;274: 13,198-13,204.
10. Schliwa M, van Blerkom J, Porter K. Stabilization of the cytoplasmic ground substance in detergent-opened cells and a structural and biochemical analysis of its composition. Proc Natl Acad Sci U S A. 1981;78:4329-4333.
11. Laemmli U. Cleavage of structural proteins during the assembly of the head of bacteriophage T4. Nature (Lond). 1970;227:680-685.
12. Kovacsovics T, Bachelot C, Toker A, et al. Phosphoinositide 3-kinase inhibition spares actin assembly in activating platelets, but reverses platelet aggregation. J Biol Chem. 1995;270:11,358-11,366.
13. Reif K, Nobes C, Thomas G, Hall A, Cantrell D. Phosphatidylinositol 3-kinase signals activate a selective subset of rac/rho-dependent effector pathways. Curr Biol. 1996;6:1445-1455.
14. Hawkins P, Eguinoa A, Qiu R-G, et al. PDGF stimulates an increase in GTP-Rac via activation of phosphoinositide 3-kinase. Curr Biol. 1995;5: 393-403.
15. Miranti C, Leng L, Maschberger P, Brugge J, Shattil S. Identification of a novel integrin signaling pathway involving the kinase Syk and the guanine nucleotide exchange factor Vav1. Curr Biol. 1998;8:1289-1299.
16. Ridley A, Hall A. The small GTP-binding protein rho regulates the assembly of focal adhesions and actin stress fibers in response to growth factors. Cell. 1992;70:389-400.
17. Ridley A, Paterson H, Johnston C, Diekmann D, Hall A. The small GTP-binding protein rac regulates growth factor-induced membrane ruffling. Cell. 1992;70:401-410.
18. Nobes C, Hall A. Rac, rho, and cdc42 GTPase regulate the assembly of multi-molecular focal complexes associated with actin stress fibers, lamellipodia, and filopodia. Cell. 1995;81:53-62.
19. Hartwig J. An ultrastructural approach to understanding the cytoskeleton. In: Carraway K, Carraway C, eds. The Cytoskeleton: A Practical Approach. The Practical Approach Series. Oxford, UK: Oxford University Press; 1992:23-45.
20. Machesky L, Mullins R, Higgs H, et al. Scar, a WASp-related protein, activates dendritic nucleation of actin filaments by the ARP2/3 complex. Proc Natl Acad Sci U S A. 1999;96.
21. Rohatgi R, Ma L, Miki H, et al. The interaction between N-WASp and the Arp2/3 complex links Cdc42-dependent signals to actin assembly. Cell. 1999;97:221-231.
22. Zigmond S, Joyce M, Yang C, Brown K, Huang M, Pring M. Mechanism of Cdc42-induced actin polymerization in neutrophil extracts. J Cell Biol. 1998;142:1001-1012.
23. Zigmond S, Joyce M, Borleis J, Bokoch G, Devreotes P. Regulation of actin polymerization in cell-free systems by GTPγS and Cdc42. J Cell Biol. 1997;138:363-374.
24. Aspenstrom P, Lindberg U, Hall A. The two GTPases, Cdc42 and Rac, bind directly to a protein implicated in the immunodeficiency disorder Wiskott-Aldrich syndrome. Curr Biol. 1996;6: 70-75.
25. Kolluri R, Tolias K, Carpenter C, Rosen F, Kirchhausen T. Direct interaction of the Wiskott-Aldrich syndrome protein with the GTPase, Cdc42. Proc Natl Acad Sci U S A. 1996;93:5615-5618.
26. Symons M, Derry J, Karlak B, et al. Wiskott-Aldrich syndrome protein, a novel effector for the GTPase CDC42Hs, is implicated in actin polymerization. Cell. 1996;84:723-734.
27. Bi E, Zigmond S. Actin polymerization: where the WASp stings. Curr Biol. 1999;9:R160-R163.
28. Miki H, Miura K, Takenawa T. N-WASp, a novel actin-depolymerizing protein, regulates the cortical cytoskeletal rearrangement in a PIP2-dependent manner downstream of tyrosine kinases. EMBO J. 1996;15:5326-5335.